

On the global and local values of the potential of zero total charge at well-defined platinum surfaces: stepped and adatom modified surfaces

Gary A. Attard^a, Omar Hazzazi^a, Peter B. Wells^a, Víctor Climent^{b,*}, Enrique Herrero^b, Juan M. Feliu^b

^a Department of Chemistry, Cardiff University, P.O. Box 912, Cardiff CF10 3TB, UK

^b Departamento de Química-Física, Universidad de Alicante, Apdo. Correos 99, E-03080, Alicante, Spain

Received 19 November 2003; received in revised form 9 February 2004; accepted 16 February 2004

Available online 24 March 2004

Abstract

N₂O reduction and CO charge displacement measurements have been used to elucidate the overall and local values of the potential of zero total charge (pztc) for a series of well-defined clean and bimetallic platinum electrodes. It is demonstrated that in all cases, analyses which incorporate measurements of surface charge (cyclic voltammetry) together with local values of the pztc (nitrous oxide reduction) to evaluate overall total charge may provide excellent agreement with overall pztc data determined using CO charge displacement. This illustrates both the veracity and consistency of both methods of pztc determination. The previous analysis reported in [J. Electroanal. Chem. 532 (2002) 67] on stepped surfaces in the [1 1 0] zone are here extended to stepped surfaces in the [0 1 1] zone, vicinal to the {1 0 0} plane. In contrast to the earlier study it is shown that the local pztc of step and terrace sites is independent of step density. For Bi adsorbed in step sites on Pt{3 3 2}, a shift to more positive values of the overall pztc relative to the clean surface is observed in agreement with predictions based on an earlier study [Electrochem. Commun. 3 (2001) 590]. The reason for this shift is discussed. Finally, the local pztc of Pd islands on Pt{1 0 0} is determined and used to calculate the variation in pztc as a function of Pd coverage. Again, good agreement with the pztc values extracted from CO displacement data is obtained. © 2004 Elsevier B.V. All rights reserved.

Keywords: Potential of zero charge; Total charge; Free charge; Platinum single-crystal; Stepped surfaces; Palladium adlayers; Bismuth adatoms

1. Introduction

The potential of zero charge (pzc) is a key parameter in electrochemistry and its importance was recognised even in the earliest studies of the electrochemical double layer using mercury electrodes [3]. Among the battery of techniques developed for the determination of the pzc of solid electrodes, the location of the minimum in the diffuse part of the differential capacity curve (based on the Gouy–Chapman–Stern model) has been among the more successful [4,5]. This method was applied to gold and silver electrodes and the influence of parameters

such as surface structure and electrolyte composition on their pzc was clearly shown and rationalised [5].

Only recently, however, have analogous studies using well-defined platinum single crystal electrodes appeared, mainly due to difficulties in their preparation and characterisation [6]. Nonetheless, the determination of the pzc of platinum single crystal electrodes is not as straightforward as in the case of gold and silver electrodes [7–12]. This is because for metals such as Pt, Pd, Rh and Ir, even the notion of double layer charge is complicated by the existence of adsorption processes associated with charge transfer and bond formation [3,13]. For such metals, in order to evaluate the “charge”, it is necessary to make additional assumptions concerning the charge distribution in the interphase. These assumptions would include the partition of electronic charge associated with chemical bond formation and electronic charge associated with the

* Corresponding author. Tel.: +44-34965903536; fax: +44-34965903537.

E-mail address: victor.climent@ua.es (V. Climent).

electrostatic attraction of the electrode surface towards electrolyte monopoles and dipoles, the so-called “free” charge [3,13]. If it is assumed, as is done generally, that the charge carried on the adsorbed ions is totally transferred to the metal side of the interphase, it is possible to distinguish between the concepts of total charge (which includes also the charge transferred during the adsorption process) and the free charge (which is the true electronic charge lying on the metal, compensated by the ionic charge in the solution). Without this assumption, it is only possible to talk about total charge, and it is not possible to determine thermodynamically its distribution in the interphase. This difference between total charge (which is the parameter usually available through experiment) and the actual free charge should be borne in mind when comparing the results obtained by different methods. Because one may distinguish between two types of charge, total and free charge, it is possible to define also two different pzcs, the potential of zero total charge, pztc, and the potential of zero free charge, pzfc.

Two methods have been applied in the last decade, among others, for the determination of the pztc by the Alicante and Cardiff groups. They are based on the recording of the current transients during potentiostatic CO adsorption [8–10] and the determination of the maximum rate of N₂O reduction [7], respectively. Both methods have given consistent values of the pztc for a variety of systems [1,7], lending support to their sensitivity to the charge stored at the interphase. In this way, the resulting values of the pztc obtained by these two methods have been compared for the three basal planes of platinum, in different electrolytes, and also platinum electrodes covered with different metal adlayers (palladium and rhodium) [7].

A fundamental difference between the two techniques is the sensitivity of the kinetics of N₂O reduction to the local characteristics of the double layer. In contrast, the CO displacement technique is an integral method that can provide a measurement only of the *overall* charge in the interphase. Consequently, the results obtained by both techniques can be compared only for homogeneous electrode surfaces (for example flat {100} and {111} terraces), while for surfaces comprised of two or more different regions (stepped or adsorbate modified), some extra considerations need to be made. In the latter case, the results obtained from the analysis of the N₂O reduction currents can be compared with the overall pztc obtained from CO displacements only if the pseudocapacities associated with the different regions of the interphase can be measured independently. We have exemplified this kind of analysis in a recent paper for the case of platinum stepped surfaces in the [110] zone [1]. The voltammograms characteristic of the electrodes in this crystallographic zone exhibit a well-defined peak associated with the electrochemical response of the step sites. This makes possible the separation of the electro-

chemical response of the steps from that of the terrace. Both contributions can be combined with their respective values of the local pztc deduced from the maximum rate of N₂O reduction to obtain an overall pztc.

In the present paper we extend the same analytical procedure to clean and bimetallic surfaces in order to demonstrate the coincidence between the results obtained using both techniques and discuss the trends observed. In addition, we seek to stress the importance of considering *local* properties of the interphase in order to understand its electrochemical behaviour completely.

2. Experimental

Single crystal electrodes were prepared from small Pt beads obtained by melting 0.5 mm diameter Pt wires (99.99%, Goodfellow Metals). The average diameter of each electrode was approximately 2.2 mm. The facets present on the surface of the beads were used to select (within 3 min of arc) the desired orientation. The electrodes were fixed, cut and polished as described previously [14]. Before each experiment, the electrodes were flame annealed, cooled in a H₂ + Ar atmosphere and quenched with water in equilibrium with the same mixture of gases. It was found that this treatment produced well-ordered surfaces [15–18].

Two methods were used to create the palladium adlayers. They can be created either by dipping the Pt{100} electrode in a diluted aqueous Pd(II) solution or by electrochemical deposition. In the first case, hydrogen was used as the reductive agent. The details of the procedure have been published elsewhere [19]. In this case, the amount of palladium deposited was controlled either through the concentration of palladium(II) in the solution (10⁻³–10⁻⁵ M) or through the deposition time (time that the surface was exposed to the hydrogen stream). In the second method, the Pd(II) is reduced electrochemically. Since the palladium concentration in the working solution is very low (10⁻⁵–10⁻⁶ M), the rate of the deposition is diffusion controlled and therefore independent of the applied potential. This allows the monitoring of the amount of deposited palladium by recording simultaneously cyclic voltammograms through the deposition process. Results by both methods are identical although the electrochemical method allows a more accurate control of the palladium coverage. In either case, it proved difficult to deposit palladium exclusively in the first monolayer for coverages >0.6 monolayers since the appearance of a second palladium peak signalled the growth of a second layer palladium [20]. To achieve palladium coverages greater than this, a selective desorption of the second layer of adatoms can be performed by adsorbing NO. The details of this procedure will be given in a separate publication [21].

Working solutions (0.1 M H₂SO₄) were prepared from concentrated sulphuric acid (Aristar or Merck Suprapur) and ultrapure water (Milipore Milli Q). The working solutions were deaerated by bubbling Ar (BOC gases or Air liquide, N50) for 15 min. Charge displacement experiments at constant potential were performed as described elsewhere [22] by dosing CO (Air liquide, N48) and N₂O (BOC gases) was used for the N₂O reduction experiments. N₂O was bubbled through the solution for 10 min to saturate the electrolyte before recording the cyclic voltammogram and a flow of N₂O was maintained above the solution at all times during the experiment.

The cyclic voltammetry equipment consisted of a wave signal generator (EG&G PARC 175), a potentiostat (Amel 551) and an X-Y-t recorder (Phillips PM 8133). A palladium wire charged with H₂ was used as the reference electrode. The potential of such a reference electrode is ca. 50 mV more positive than the reversible hydrogen electrode. The counter electrode was a coiled Pt wire immersed in the same working compartment. All experiments were performed at room temperature.

3. Results and discussion

3.1. Platinum stepped surfaces

The existence of different local values of the work function on step and terrace sites for stepped surfaces has been stressed several times in UHV studies. The use of techniques such as photoemission of adsorbed xenon (PAX) [23] and STM [24] has allowed the determination of local values of the work function. It has been observed that the local work function of the step sites is in general lower than that of the terrace sites. This effect has usually been explained by considering the behaviour of surface dipoles close to the step sites due to the so-called Smoluchowski effect [25]. This effect arises because the electronic cloud in the metal does not follow the abrupt change of positive charges near the steps. This causes the appearance of positive charges on the upper part of the steps and negative charges on the lower side of the steps. The resulting separation of charges between the lower and upper part of the step creates a dipole in opposition to the normal surface dipole associated with the spillover of the electronic cloud into vacuum, thereby locally lowering the work function near step sites. This effect has long been known and used to explain the linear decrease of the work function with the increase of the density of steps or defects on the surface of metals [26], although its direct determination was made possible only later with the PAX and STM techniques mentioned above.

The analogous existence of local values of the pzc in the electrochemical environment has been suggested for stepped gold [5,27] and platinum [7,9,10] electrodes. In the latter case, one has to consider the possible existence of local values for both the pztc and the pzfc. The existence of more negative values of the pztc for step sites on platinum stepped surfaces in the [1 $\bar{1}$ 0] and [01 $\bar{1}$] crystallographic zones was suggested by the Alicante group to explain the decrease of the overall pztc calculated from the charges displaced during CO adsorption [9,10]. This decrease in the pztc was also related to a similar decrease in the pzfc [10], although the latter parameter can be determined only through a rather risky extrapolation of the charge vs. *E* curve into the hydrogen region.

Independently of the CO displacement measurements, the observation of two local maxima in the N₂O reduction currents with defective surfaces was taken by the Cardiff group as an indication of the sensitivity of this reaction to the local distribution of charges on the electrode surface [7]. Lately, the consistency between the pztc values obtained with CO displacement and from the location of the N₂O reduction maxima was demonstrated for the platinum stepped surfaces in the [1 $\bar{1}$ 0] zone [1]. In this section, we complement the analysis made in [1] with the stepped surfaces in the [01 $\bar{1}$] zone, vicinal to the {100} plane. This particular choice for the geometry of the electrodes is conditional on the necessity of having well separated voltammetric contributions corresponding to terrace and step sites, needed for the determination of the charges associated with both surface sites.

Fig. 1 shows cyclic voltammograms in 0.1 M H₂SO₄ corresponding to platinum stepped surfaces in the [01 $\bar{1}$] zone. The voltammograms in the top half of the graph, from Pt{2311} to Pt{311}, correspond to surfaces composed of {100} terraces separated by {111} monoatomic steps. Their surface structure can be written as Pt(S)[*n*(100) × (111)], with terrace width, *n*, spanning seven to two atomic rows, respectively. The cyclic voltammogram corresponding to the Pt{100} electrode surface is included at the top of Fig. 1, since it would correspond ideally to an infinitely wide terrace. Also, the voltammograms corresponding to three stepped surfaces with {111} terraces and {100} steps (Pt{211}, Pt{533} and Pt{755}) and the Pt{111} surface have been included in the bottom half of the same graph. In all cases, there is good agreement between the voltammograms in Fig. 1 and those reported previously for the same surfaces [14,28–30], if allowance is made for the different electrolyte concentrations.

Let us focus first on the voltammograms corresponding to surfaces with {100} terraces. Several peaks are observed in these voltammograms. They have been assigned to hydrogen and anion adsorption in the surface sites of different geometries [29,31]. From the trend

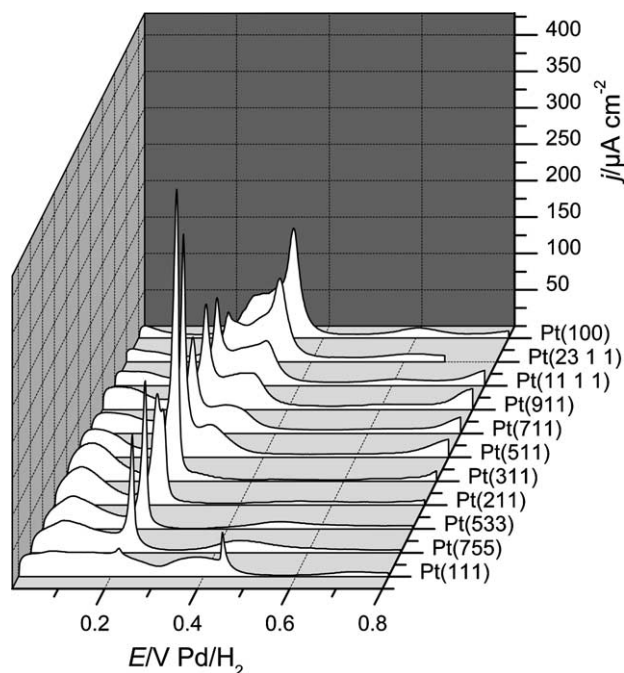


Fig. 1. Cyclic voltammograms corresponding to platinum stepped surfaces in the $[01\bar{1}]$ crystallographic zone in 0.1 M H_2SO_4 . Sweep rate: 50 mV s^{-1} .

observed when the terrace width is shortened it is possible to assign the voltammetric current at potentials $<0.15 \text{ V}$ and the sharp peak at 0.22 V to the electrochemical responses associated with the steps. On the other hand, the decrease of the voltammetric features at potentials $>0.25 \text{ V}$ when the density of steps is increased allows us to assign this current to the response associated with terrace sites.

In order to understand the nature of the two processes associated with adsorption on steps, comparison can be made with the voltammograms of the other series of stepped surfaces in the same crystallographic zone: $\text{Pt(S)}[n(111) \times (100)]$. The intersection between both series of stepped surfaces coincides with the $\text{Pt}\{311\}$ surface which can be understood either as $\text{Pt(S)}[2(111) \times (100)]$ or $\text{Pt(S)}[2(100) \times (111)]$. For this series, a peak at 0.22 V is also observed and has been ascribed to hydrogen adsorption on $\{100\}$ step sites. Voltammetric contributions $<0.2 \text{ V}$ in this series of stepped surfaces have been ascribed to hydrogen adsorption on the $\{111\}$ terraces. Both conclusions are supported by the analysis of the voltammetric charges [30]. Once the turning point of the crystallographic zone is reached, the $\{111\}$ terraces become the $\{111\}$ steps. Therefore, the currents at potentials $<0.15 \text{ V}$ in the voltammograms of electrodes with the $\text{Pt(S)}[n(100) \times (111)]$ structure can be assigned to hydrogen adsorption on $\{111\}$ steps. On the other hand, the $\{100\}$ steps in the $\text{Pt(S)}[n(111) \times (100)]$ stepped surfaces would become the step edge in the $\text{Pt(S)}[n(100) \times (111)]$ series.

This argument allows us to assign the peak at 0.22 V to adsorption processes on the terrace atomic row adjacent to the step sites.

The previous conclusion is further supported by the analysis of the integrated charges under the voltammetric currents and their comparison with the number of sites of different geometry deduced from the ideal hard sphere model of the surface. According to the previous arguments, three regions can be defined in the voltammograms of Fig. 1: below the minimum around 0.15 V , between this minimum and the minimum around 0.25 V , just above the peak, and the region above this point (we have taken the upper limit of integration as 0.7 V). The charges under these three regions would correspond to the contributions from the $\{111\}$ step, the step edge and the terrace, respectively. These parameters have been plotted against the step density in the graph shown in Fig. 2. The step density, defined as the number of step sites per unit length in the direction perpendicular to the step, is given by

$$N = \frac{1}{d(n-1/2)}, \quad (1)$$

where d is the atomic diameter of platinum. It is clear from this plot that the charges under different regions follow a linear dependence versus the step density. A similar analysis of the voltammetric charges obtained with platinum electrodes in the same crystallographic zone was performed in [31].

The charges deduced from the hard sphere model have also been plotted in Fig. 2. The surface of the unit cell is given by¹

$$S = d^2(n-1/2). \quad (2)$$

If we consider that there is only one step site per unit cell, the charge corresponding to one electron transfer per step site is given by

$$q_{\text{step}} = \frac{e}{d^2(n-1/2)}. \quad (3)$$

The assumption that the peak at 0.22 V corresponds to adsorption on the step edge, forces us to assume that only $(n-2)$ sites are available per unit cell for adsorption on the terrace sites, leading to the following ex-

¹ In this expression, S is the surface projected on the plane of the terrace, i.e., the $\{100\}$ plane. However, the current densities in the voltammograms of Fig. 1 are referred to the geometric area of the electrode surface. In order to compare with the values given by the hard sphere model, the charges integrated from the voltammogram should be projected on the plane of the terrace by dividing through the cosine of the angle between both planes. This is given by

$$\cos \alpha = \frac{n-1/2}{\sqrt{(n-1/2)^2 + 1/2}}.$$

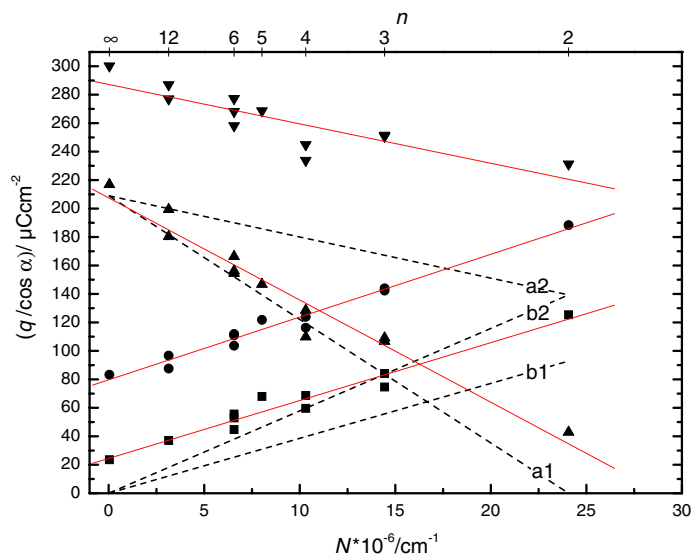


Fig. 2. Plot of the integrated voltammetric charges against the step density for the surfaces vicinal to the $\{100\}$ plane. (■) Between 0 and 0.13 V; (●) between 0.13 and 0.25 V; (▲) between 0.25 and 0.70 V; (▼) between 0.13 and 0.70 V. Solid lines are best fits to the charges in the different regions. Dashed lines correspond to the charges predicted by the hard sphere model of the surface, according to Eqs. (3), (4a) (curve a1) and (4b) (curve a2) with $\theta_{\max} = 2/3$ (curve b1) and $\theta_{\max} = 1$ (curve b2). Voltammetric charges are referred to the surface projected on the plane of the $\{100\}$ terrace. See text for details.

pression for the charge corresponding to one electron per terrace site:

$$q_{\text{terrace}} = \frac{(n-2)e}{d^2(n-1/2)} = q_{100} - \frac{(3/2)q_{100}}{d^2(n-1/2)}, \quad (4a)$$

where $q_{100} = e/d^2 = 209 \mu\text{C cm}^{-2}$, corresponds to the charge associated with the transfer of one electron per surface site on the ideal $\text{Pt}\{100\}$ - (1×1) surface. Should $(n-1)$ sites be available for adsorption on terrace sites, the following expression would be obtained:

$$q_{\text{terrace}} = \frac{(n-1)e}{d^2(n-1/2)} = q_{100} - \frac{(1/2)q_{100}}{d^2(n-1/2)}. \quad (4b)$$

The increase of the step contribution below 0.15 V is roughly consistent with the transfer of one electron per step site. However, one consideration can be made here, since the maximum hydrogen coverage on the $\text{Pt}(111)$ terraces has been shown to be $2/3$ monolayers [32]. Then, if the same maximum coverage is conserved as we move along the $[01\bar{1}]$ zone and the (111) terrace becomes the $(1\bar{1}1)$ step, a constant factor θ_{\max} should be inserted in Eq. (3). This factor, expected to be ≤ 1 , would cause a decrease of the slope of the plot of the charge associated with the steps vs. step density (Fig. 2). The resulting curves obtained with the extreme values of $\theta_{\max} = 2/3$ and $\theta_{\max} = 1$ are plotted in Fig. 2, curves b1 and b2, respectively. From this plot we can conclude that the slope of the experimental points agrees better with the values predicted with $\theta_{\max} = 2/3$. Another point that needs discussion is the existence of a non-zero interception with the y-axis of the line extrapolated from

the experimental points. We can propose the existence of a non-negligible density of steps on the $\{100\}$ surface as a tentative explanation for this non-zero intercept. Those defects would arise during the lifting of the hexagonal reconstruction that is likely to take place at the high temperatures achieved during the flame annealing treatment. The reconstruction would be removed by hydrogen electrosorption when the electrode is contacted with the solution in the hydrogen underpotential deposition range [16,33]. This effect can be diminished by cooling the electrode after the flame annealing in a hydrogen-containing atmosphere [18]. In this way, the reconstruction is likely to be lifted at higher temperature, which would facilitate a better reordering of the surface atoms to accommodate the extra atoms that must be expelled from the surface during the lifting of the reconstruction. At present, however, all $\text{Pt}\{100\}$ voltammetric profiles reported in the literature show contributions in this low potential region. The previous argument can explain the existence of voltammetric contributions in the potential region associated with steps for surfaces with wide $\{100\}$ terraces (i.e., low step density, $n > 15$ [31]). Another cause for the observation of charge in this potential region could be the initial stages of hydrogen evolution. Finally, it must be stressed that charges plotted in Fig. 2 are measured without any double layer correction. If we consider the average double layer capacity in each potential region as independent of the step density, the double layer correction would imply a vertical displacement of all the points in Fig. 2 by an equal amount, therefore, leaving unchanged

the slope of the different lines. However, this effect is not enough to explain the non-zero intercept of the line corresponding to the charge on step sites.

The charges under the sharp peak at 0.22 V increase parallel to the contribution of the steps. This supports their assignment to adsorption processes on terrace atoms at the edge of the steps. It is worth pointing out that the charges measured in this region do not correspond to a single process, but include both hydrogen adsorption and anion desorption, as revealed by charge displacement experiments with CO and spectroscopic data [31].

Another piece of information can be obtained from the analysis of the decrease of the charge assigned to adsorption on the terraces with the step density. This decrease is more consistent with $(n - 2)$ adsorption sites per terrace (Eq. (4a)) than with $(n - 1)$ (Eq. (4b)), giving additional support to the assignment of the charges under the peak to adsorption on the row of atoms adjacent to the step. Again, one has to bear in mind that the charge measured in this region corresponds to more than a single process and therefore, what is important in this plot is the comparison of the gradients and not the actual values of charge.

The current density in the voltammograms of Fig. 1 can be integrated in order to obtain a graph of total charge vs. potential. However, the integrated curve contains an undetermined integration constant that needs to be evaluated independently in order to locate the relative position of the curve. This integration constant can be obtained from the charge displaced during CO adsorption at a given potential, according to [8]

$$q(E) = \int_{E^*}^E \frac{|j_v|}{\nu} dE - q_{\text{dis}}(E^*), \quad (5)$$

where j_v and ν are the voltammetric current density and the sweep rate, respectively, and E^* is the potential of the CO charge displacement experiment. This approach was followed for these surfaces in perchloric acid solution in the absence and in the presence of sodium acetate [31].

Alternatively, the relative vertical position of the integrated curve can be determined from the local values of the pztc deduced from the N_2O reduction currents. Fig. 3 shows voltammetric current when N_2O is present in the solution, for different stepped surfaces. This figure clearly demonstrates the existence of two N_2O reduction maxima at 0.22 and 0.34 V. The evolution of the maximum current of these peaks with the introduction of steps allows one to assign them to N_2O reduction on step edges and terrace sites, respectively. This is also supported by the coincidence between the N_2O reduction currents and the peak potentials in the voltammograms of Fig. 1. Remarkably, for $\text{Pt}(S)[n(100) \times (111)]$ stepped surfaces the potential of the maximum reduction current is constant for electrodes with different step densities (see later). It is noteworthy that there is also a

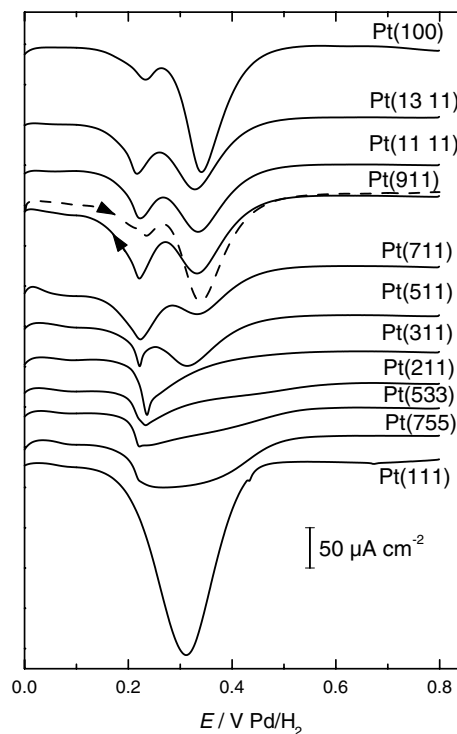


Fig. 3. Voltammetric current corresponding to different platinum stepped surfaces in the $[01\bar{1}]$ crystallographic zone in 0.1 M H_2SO_4 solution saturated with N_2O . Sweep rate: 5 mV s^{-1} .

very weak N_2O reduction peak at 0.08 V that could be associated with reduction on step sites.

If we identify the location of the N_2O reduction maxima with the local pztc of the steps, step edges and terrace sites, we can combine them with the integrated curves from the different regions of the voltammograms in order to obtain their respective integration constants. Then, the curves for the different regions can be added to obtain the overall curve of charge versus potential, from which the overall pztc can be read from its interception with the potential axis. This can be compared with the curve obtained by using the integration constant from the displaced charge with CO.

The procedure is exemplified in Fig. 4 for one particular stepped surface, $\text{Pt}\{11\bar{1}1\}$, which corresponds to a nominal terrace width of six atomic rows. Fig. 4(B) shows the voltammetric currents with and without N_2O in solution, and has been included as a visual reference for the potential scale. Fig. 4(A) contains the integrated curves for the contribution from the steps, the step edges and the terraces. The vertical lines in Fig. 4(A) indicate the limits of the integration regions (dashed lines) and the position of the local pztc (dotted lines), as inferred from the maxima in the reduction current. One simplification that has to be done in this analysis concerns the separation of the double layer charge for the different regions. These contributions cannot be separated as straightforwardly as the contributions from the ad-

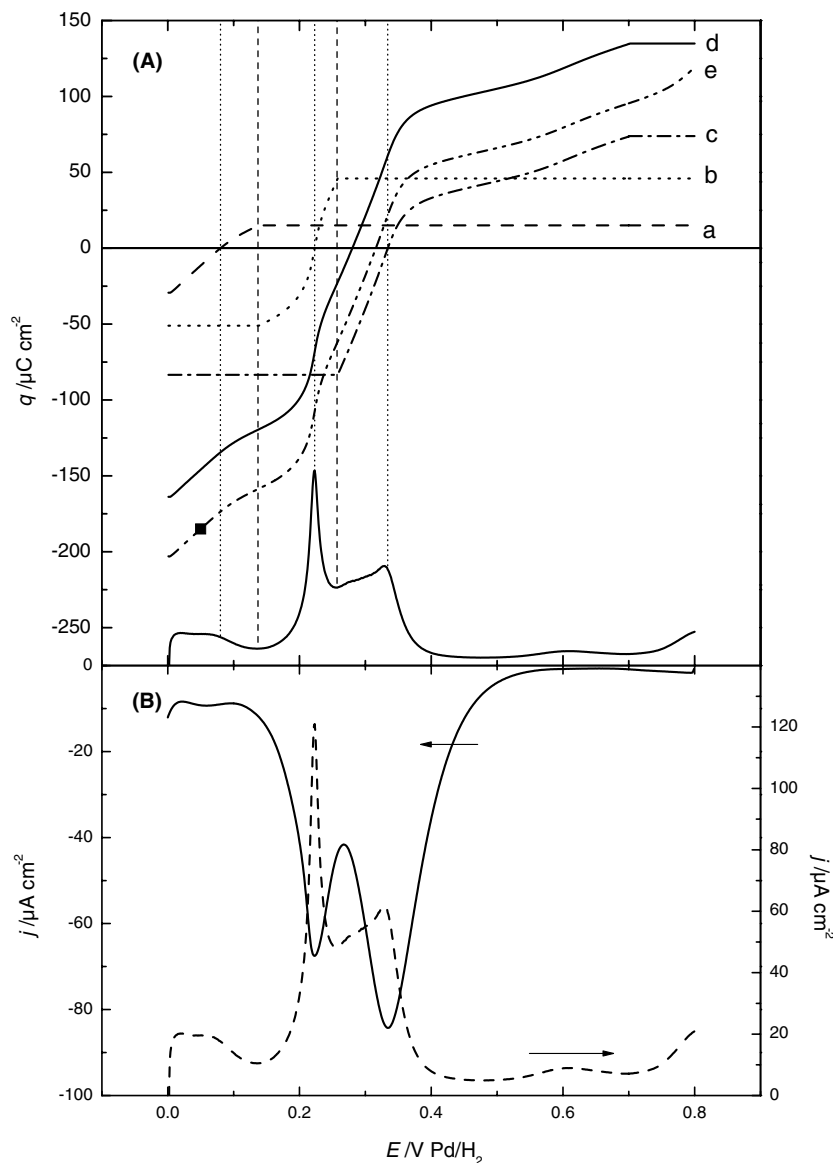


Fig. 4. (A) Different charge contribution obtained from the integration of the current density on the different regions of the voltammogram corresponding to a Pt{111} electrode surface: (a) steps; (b) step edge; (c) terrace; (d) overall charge obtained as the sum of curves a–c; (e) overall charge obtained using the CO displaced charge at 0.06 V as the integration constant. Vertical lines mark the position of the integration limits (dashed) and the local pztc (dotted). (B) Voltammetric current corresponding to the Pt{111} surface in 0.1 M H₂SO₄ with (solid line) and without (dashed line) N₂O. Sweep rate: 5 and 50 mV s⁻¹, respectively.

sorption processes. As a first approximation, any double layer correction has been neglected in the analysis. This relies on the fact that adsorption processes represent the main contribution to the total charge. As a result, the total charge for the different parts of the surface is considered as constant outside the potential range where the adsorption process takes place. The true curve would increase slightly, with a slope corresponding to the double layer capacity for each region. We have tentatively attempted to correct the curves with constant values of the double layer capacity, proportional to the number of sites of each type, without significant changes in the resulting values of the pztc.

Once the integrated curves for the different potential regions have been adjusted vertically by using the local values of the pztc, the overall total charge vs. potential curve can be obtained simply by their summation. Finally, the overall pztc can be read as the intercept of the resulting curve with the potential axis.

Fig. 5 shows the resulting values of the pztc for the different surfaces studied. The values are compared also with those obtained from CO displacement experiments. There is a clear correlation between the results obtained by both methods. There is an almost linear decrease of the pztc with the increase of the step density, except for the highest step density. As discussed earlier, this

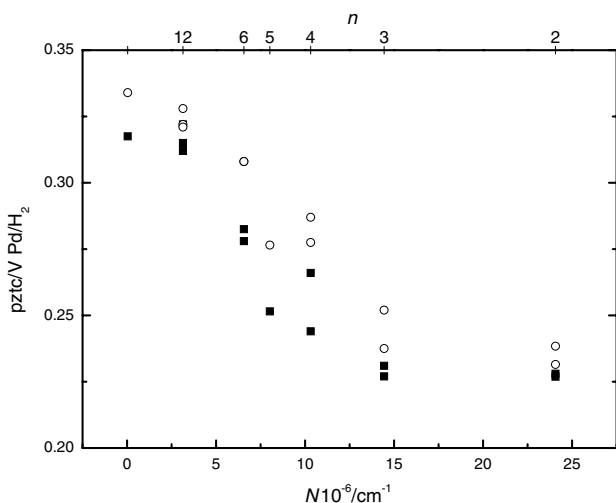


Fig. 5. Plot of the overall pztc versus the step density, as obtained from the analysis using local values of the pztc from N_2O (squares) and the CO displaced charge (open circles).

decrease can be explained in terms of the Smoluchowski effect, or the appearance of dipoles on step sites, causing a decrease of the overall surface potential.

3.2. Stepped surfaces covered with bismuth

Another example in which N_2O reduction can be used to locate the local pztc is in the case of stepped surfaces decorated with adatoms. It has been shown that stepped surfaces vicinal to the $\{111\}$ crystallographic orientation can be decorated with certain adatoms in such a way that the adatom is deposited initially on step sites and the deposition on the $\{111\}$ terrace sites does not start until the step sites are completely blocked [34]. It has also been shown that only adatoms of elements more electropositive than platinum (with lower work function, i.e., Bi, As, Te) are able to adsorb selectively on step sites while more electronegative adatoms, like selenium and sulphur, adsorb both on terraces and steps without any selectivity. The possibility of decorating step sites with adatoms poses an intriguing question concerning the effect of such controlled modification of the surface on the overall pztc.

In a previous publication it has been shown by using the CO displacement technique that the pztc of the stepped surface shifts toward more positive values when the step sites are selectively blocked with bismuth adatoms [2]. This shift of the pztc is remarkable because it opposes the expected trend that one would predict from the variation of the work function due to bismuth adsorption in UHV [35]. A similar conclusion is obtained from the determination of the local pztc of the stepped surface with and without bismuth as we show in the following.

Fig. 6 shows the analysis performed by using the local pztc obtained from the N_2O reduction currents on a Pt $\{332\}$ stepped surface with and without bismuth. Fig. 6(A) shows the positive sweep of the voltammogram corresponding to this surface in 0.1 M H_2SO_4 (curve a). Also in this figure are shown the different contributions attributed to terrace and step sites (curves b and c, respectively). Finally, the dashed line (curve d) in Fig. 6(A) corresponds to the surface selectively covered with bismuth adatoms deposited on the step sites. In this curve it can be clearly seen that, while adsorption on step sites is completely blocked by the bismuth, the voltammetric contribution from the terrace sites is nearly the same as that of the clean surface.

Fig. 6(B) shows the N_2O reduction currents on the clean (a) and on the bismuth modified (d) surface. Two reduction maxima are observed on the curve corresponding to the clean surface at ca. 0.07 and 0.23 V, which have been previously considered as indicative of the location of the local pztc of the step and the terrace, respectively. Following the approach described in [1] and outlined above, these local values of the pztc can be combined with the integration of the different contri-

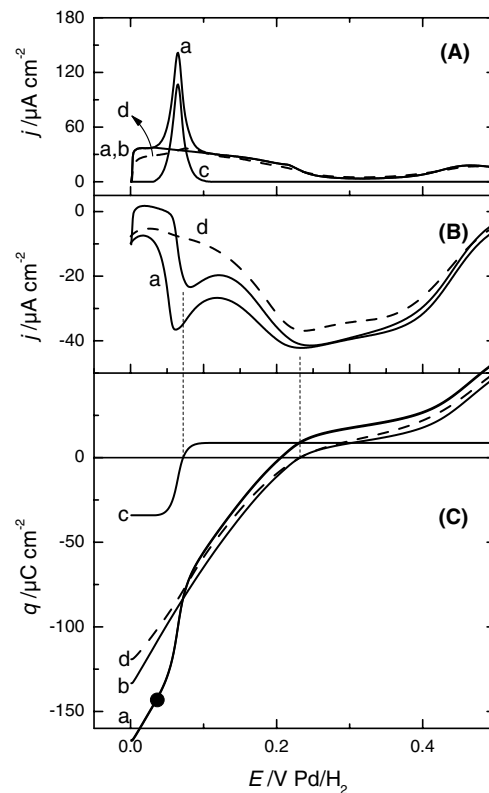


Fig. 6. Cyclic voltammograms corresponding to a Pt $\{332\}$ stepped surface in 0.1 M H_2SO_4 solution without (A) and with (B) N_2O and charges integrated from the voltammetric currents (C). Curves a and d correspond to the clean and the bismuth modified surface, respectively, while curves b and c refer to the terrace and step contributions for the unmodified surface.

contributions to the voltammetric current from the terrace and step sites in order to obtain the overall pztc corresponding to the whole surface. Fig. 6(C) shows the resulting curves. Curves b and c correspond to the contribution from the terrace and step sites, respectively. They have been obtained by integrating voltammetric currents b and c in Fig. 6(A). Curve a has been obtained by adding curves b and c and corresponds to the total charge on the surface. It is clear that the overall pztc lies between the local pztc of the terrace and the step. For the sake of comparison, the total charge obtained at 0.04 V from CO displacement is indicated as a solid circle in Fig. 6(C). An excellent agreement is observed in this case between the charges obtained from the CO displacement method and those inferred from the analysis of the N₂O reduction current.

When step sites are covered with bismuth, the maximum in the N₂O reduction current attributed to the step at 0.07 V disappears while the rest of the curve remains almost unmodified (curve d in Fig. 6(B)). Remarkably, the position of the maximum current attributed to the location of the local pztc of the terrace remains unchanged, stressing the local character of the terrace and step contributions. In this case the local pztc deduced from the N₂O reduction coincides with the overall pztc of the modified surface. Comparison of the curves a and d in Fig. 6(C) shows a positive shift of the pztc after modification of the surface by bismuth deposition in good agreement with the previous conclusion extracted from the CO displacement measurement.

3.3. Palladium adlayers on Pt{100}

It has been shown that palladium forms epitaxial adlayers on platinum and gold substrates. These adlayers can be grown either in ultra high vacuum or by conventional electrochemical methods. The possibility of readily preparing palladium adlayers by electrochemical methods and the well-ordered nature of these adlayers have drawn much attention to this system over the last decade from the electrochemical community [19,20,36–49]. Moreover, the fact that, for submonolayer coverages, the surface is composed of palladium islands and free platinum sites, both exhibiting well-separated electrochemical responses, allows an easy characterisation of these adlayers by electrochemical methods, e.g., cyclic voltammetry [20].

Fig. 7 contains cyclic voltammograms for a Pt{100} electrode surface covered with different amounts of Pd in 0.1 M H₂SO₄. The starting cyclic voltammogram corresponding to the unmodified Pt{100} electrode is included again in Fig. 7. The effect of palladium deposition on the cyclic voltammogram is clearly evident as a very sharp peak at ca. 0.125 V. This peak grows as the amount of deposited palladium is increased, while the platinum contributions at potentials >0.13 V decreases.

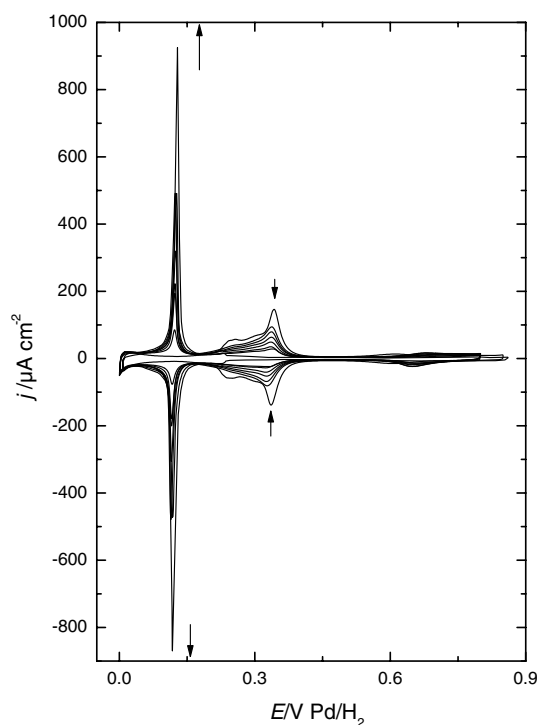


Fig. 7. Cyclic voltammogram corresponding to a Pt{100} electrode covered with submonolayer amounts of palladium. The palladium coverages, following the direction of the arrows are: 0, 0.11, 0.24, 0.30, 0.40, 0.60, 0.66 and 0.99 ML, calculated as described in the text. The last two voltammograms are taken from [50].

It has been shown previously that the palladium coverage can be easily calculated from the charge under the voltammetric peak at 0.125 V, by dividing this charge by its maximum value when the surface is totally covered by palladium (ca. 240 $\mu\text{C cm}^{-2}$) [21,50].

Fig. 8 shows the positive scans of the cyclic voltammograms obtained for exactly the same partially Pd-covered surfaces when the solution is saturated with N₂O. Two reduction maxima appear in the voltammogram for the partially covered surfaces, one at ca. 0.34 V and the other exactly at the same palladium peak position at 0.125 V. The cyclic voltammograms in the absence of N₂O for the bare surface and for $\theta_{\text{Pd}} = 1$ have been included in Fig. 8 as a reference. The evolution of the N₂O reduction current with the change in the amount of palladium allows one to assign the maximum at 0.125 V to the palladium contribution while reduction at a more positive potential would originate from free platinum surface sites.

According to the previous discussion, the potential of the N₂O maximum corresponds to the position of the local pztc [1,7]. Therefore, the existence of two maxima in the voltammograms in Fig. 8 suggests the existence of two local pztcs, one corresponding to the palladium covered regions of the surface (at ca. 0.125 V) and the other corresponding to the residual platinum free sites

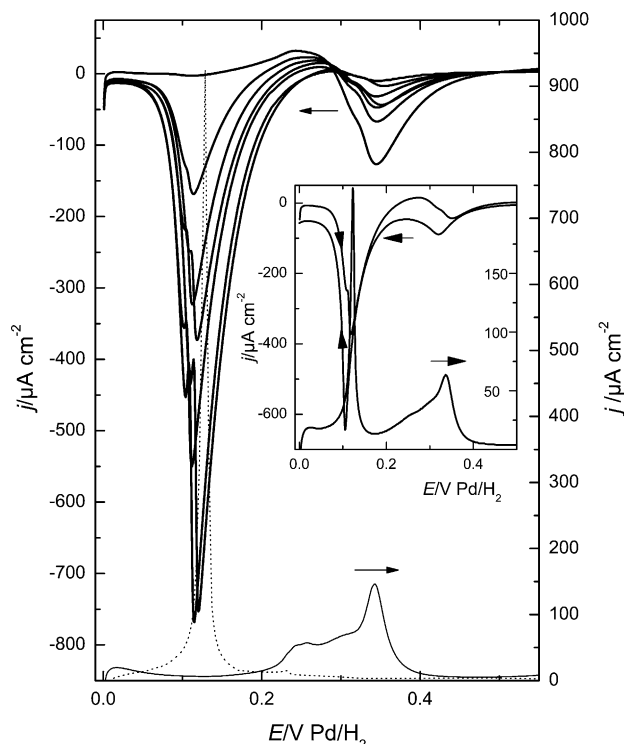


Fig. 8. Positive sweep of the cyclic voltammogram obtained in 0.1 M H_2SO_4 solutions saturated with N_2O for a Pt{100} electrode with different Pd coverages: 0, 0.11, 0.24, 0.30, 0.40, 0.60, 0.63 ML. The positive sweep of the voltammogram obtained in the absence of N_2O for the clean and the totally covered Pt{100} electrode are shown for the sake of comparison. Inset: Positive and negative sweep for the Pt{100} electrode covered with 0.30 ML of palladium.

(ca. 0.34 V). The position of both local pztc's remains approximately constant as the palladium coverage is changed. As we did with the stepped surfaces, the position of this local pztc can be used as an origin for the integration of the palladium and platinum contributions in the voltammogram.

However, before doing this, there is a point that is worth noting: there is some hysteresis in the position of the N_2O reduction maxima. To show this behaviour, the complete cyclic voltammogram (positive and negative sweeps) for an intermediate Pd coverage ($\theta_{\text{Pd}} = 0.3$) is given in the inset of Fig. 8. As before, the positive sweep without N_2O in solution is included as a guide to the potential scale. Clearly, both maxima in the N_2O reduction current are located slightly more negative in the negative sweep than in the positive scan. Although the difference in the peak potentials is very small, it can be significant when its location, identified with the local pztc, is used to define the integration constant to obtain the local charge corresponding to the areas covered with palladium. Since the peak corresponding to palladium islands is very sharp, its integration gives a very steep increase of the charge and hence a small shift in the local pztc would change the charge from being mainly nega-

tive to mainly positive. In this regard, the maximum in the negative sweep for N_2O reduction is located at more negative potentials than the palladium peak (see inset in Fig. 8). This would imply that the charge corresponding to these peaks is mainly positive (mainly anion adsorption). On the other hand, the maxima for the positive N_2O reduction sweeps almost coincide with the potentials of the palladium peak. Since this peak is asymmetric, the latter location of the local pztc implies that around two-thirds of the charge under the peak would correspond to negative charge and one-third of the peak to positive charge. The latter makes most sense and agrees with the results obtained with the CO displacement technique [21,50]. We can understand the hysteresis as an effect of the strong anion adsorption in the palladium islands, which would need a slightly negative overpotential to be completely desorbed. This would lead to a kinetic effect not desirable for the analysis of the thermodynamic charges. For this reason we chose to use the value of the local pztc deduced from the positive sweep of the N_2O reduction.

Fig. 9 illustrates the procedure used to separate the contributions in the voltammogram corresponding to the palladium covered and palladium free areas of the electrode, similar to what has been done previously for the stepped platinum surfaces. According to the previ-

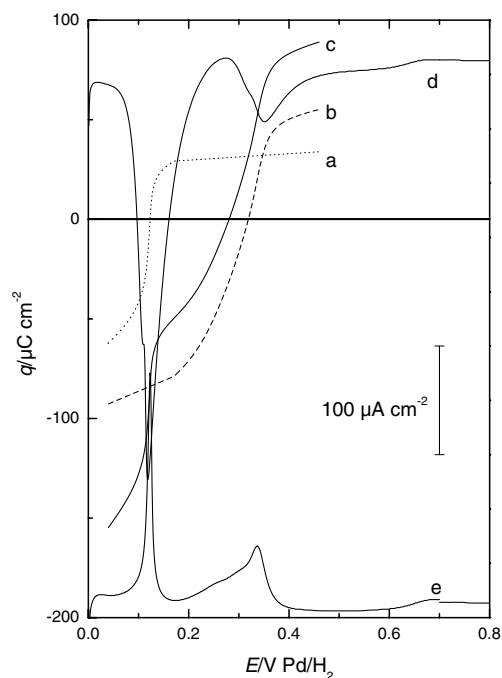


Fig. 9. Different charge contributions obtained from the integration of the current density on the different regions of the voltammogram corresponding to a Pt{111} electrode covered with 0.30 monolayers of palladium. (a) Palladium contribution. (b) Platinum contribution. (c) Overall charge obtained as the sum of curves a and b. The positive sweeps of the voltammogram obtained with and without N_2O for the same electrode are shown for the sake of comparison.

ous discussion, the charge integrated between 0.03 and 0.180 V corresponds to the palladium contribution to the overall total charge, and the contribution at higher potential would correspond to the uncovered platinum regions. Again, the separation of the double layer contributions is not straightforward. However, in this case the double layer capacity of the palladium and platinum areas can be determined from their values for the Pt{1 0 0} and the totally covered Pd/Pt{1 0 0} electrodes, if we consider them as constants as a function of potential and palladium coverage. Then, a constant double layer capacity proportional to the palladium coverage was considered to separate the voltammetric currents for both the palladium and platinum regions. According to this, the charge integrated in the first region between 0.03 and 0.18 V has been corrected to take account of the double layer contribution from the uncovered platinum areas. The double layer capacity for performing this correction is estimated as:

$$C_{\text{dl}}^{\text{Pt}} = C_{\text{dl}}^{\text{Pt},\theta=0}(1 - \theta_{\text{Pd}}), \quad (6)$$

where $C_{\text{dl}}^{\text{Pt},\theta=0}$ stands for the apparent average capacity of the double layer in this potential region corresponding to a Pd-free electrode (ca. $140 \mu\text{F cm}^{-2}$).

Similarly, the charge integrated between 0.18 and 0.46 V corresponds to the Pd-free contributions. Again, this charge should be corrected to take into account the double layer contribution of the palladium covered regions in this potential range

$$C_{\text{dl}}^{\text{Pd}} = C_{\text{dl}}^{\text{Pd},\theta=1}\theta_{\text{Pd}}, \quad (7)$$

where an apparent $C_{\text{dl}}^{\text{Pd}}$ was measured as ca. $55 \mu\text{F cm}^{-2}$.

In order to adjust the local pztc, both curves, corresponding to the Pd free and Pd covered regions, are shifted vertically to match the interception of the curve with the x-axis and the position of the local pztc. The latter is obtained from the maxima in the N_2O reduction currents, as stated above. However, to overcome the problem arising from the hysteresis observed between the positive and negative sweeps as discussed above, the peak potential at 0.125 V was taken as the local pztc for the palladium contribution, which coincides with the maximum N_2O reduction current during the positive sweep. This seems the most reasonable assumption and gives the better agreement with the global pztc obtained from the CO displacement. Again, to set the local pztc for the Pt regions, we need to choose either the positive or negative sweep. The position of the maximum N_2O reduction current in the positive sweep was used in the example shown in Fig. 9, although both the local pztcs extracted from the positive and negative sweeps have been used and the results averaged in Fig. 10.

The global potentials of zero charge are compared with those obtained with the CO displacement in Fig. 10. The fit between both sets of data is rather good with both the general trend and absolute value of pztc

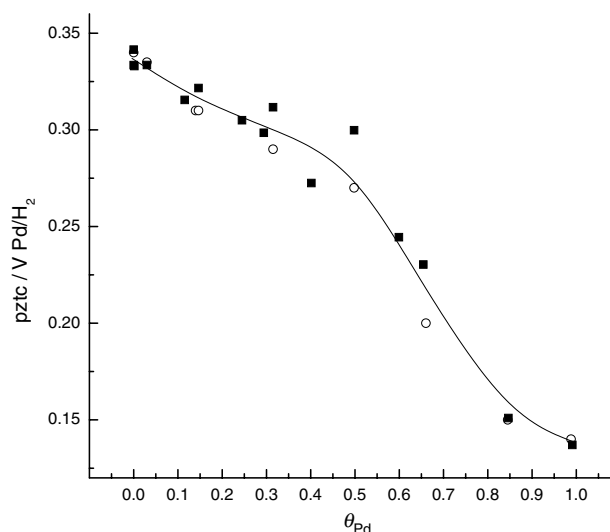


Fig. 10. Plot of the overall pztc versus the palladium coverage, as obtained from the analysis using local values of the pztc from N_2O (■) and the CO displaced charge (○).

being reproduced over the entire coverage range of palladium studied.

3.4. Overview of CO charge displacement and nitrous oxide reduction as probes of double layer structure

In the present study, three different adsorption systems, namely stepped surfaces in the $[01\bar{1}]$ zone, bismuth decorated steps of Pt{3 3 2} and Pd/Pt{1 0 0} have been investigated in order to test the efficacy of measuring local pztc data (via nitrous oxide reduction) and converting such data into “global” pztc values comparable with information obtained via CO charge displacement. That in all cases the congruence between both methodologies is good, as was found previously for adsorption on Pt single crystal electrode surfaces in the $[1\bar{1}0]$ zone [1] lends further support to the ability of both methods to evaluate the charged state of the interface. Both approaches are physically quite independent of each other, yet each provided consistent values of pztc.

For the stepped surfaces in the $[01\bar{1}]$ zone an almost linear decrease in pztc with step density is attributable to a Smoluchowski effect. In contrast to stepped surfaces in the $[1\bar{1}0]$ zone [1], in the present study, the local values of the pztcs of step and terrace sites remained constant irrespective of step density. It is speculated that this effect is associated with differences in the capacitance of the terrace adjacent to the step. For example, it has already been mentioned that the dipole that forms at step sites is caused by a localised charge displacement in response to the atomic geometry of the step. If this charge is displaced onto the terrace, the amount of charge that can be accommodated there must be a function of the capacitance of the terrace as a function of potential. If

this value was relatively low and was exceeded at high step densities (when the total amount of displaced charge from the step onto the terrace is at its highest), it may be expected that charge may return to the step leading to a shift in its local pztc. Similarly, as the step density increases, the local pztc of the terrace would also shift in response to its limit in accommodating excess charge being reached. This is essentially what was found for the local pztc values of terrace and step in the $[1\bar{1}0]$ zone [1]. However, if the terrace exhibits a larger capacitance, then little perturbation in the local pztc of step and terrace is predicted as a function of step density since the displaced charge from the step, even at high step densities is insufficient to alter the pztc value of the adjacent terrace. This is the behaviour observed in the present study and therefore it is asserted that, at a fixed potential, the surface dipoles at terraces and steps remain constant with increasing step density leading to constant values of the local pztc. Unfortunately, the application of the arguments above to the present case is complicated by the fact that we are dealing with total charge instead of with free charge and there is also a component due to ionic adsorption. This component has a buffering effect on the changes of the local pztc, since it increases the ability of the interface to store larger amounts of charge [10]. This buffering effect is increased when the pseudocapacity of the adsorption process is large i.e., Pt{100} sites in comparison with Pt{111}.

For Pt{332}, the decoration of $(111) \times (111)$ step sites by bismuth caused a shift of the overall pztc to more positive potentials in accordance with expectations based on previous electrochemical investigations [2]. The use of nitrous oxide reduction as a local probe of pztc provides a simple reason for this shift. Remember that because $\text{pztc}(\text{step}) < \text{pztc}(\text{terrace})$, for potentials V in the range $\text{pztc}(\text{step}) < V < \text{pztc}(\text{terrace})$ the steps will bear a positive total charge whereas the terraces will simultaneously bear a negative total charge. The net sum of these total charges will be zero at the value of the overall pztc (when CO displaces all components of the double layer). Hence, for clean Pt electrode surfaces

$$\text{pztc}(\text{step}) < \text{overall pztc} < \text{pztc}(\text{terrace}). \quad (8)$$

If the transient current contribution from steps is no longer present due to steps being blocked by bismuth, it means that there is only displacement from residual {111} terrace sites and hence in this case

$$\text{overall pztc} = \text{pztc}(\text{residual terrace sites}). \quad (9)$$

Confirmation of the disappearance of a local $\text{pztc}(\text{step})$ and the “unperturbed” nature of the residual {111} terraces comes from inspection of Fig. 6(B) whereby the clean and bismuth-modified surfaces display identical N_2O reduction behaviour save for the step region of the voltammogram. The question then arises, is there any stored charge at bismuth adatoms? Does the

Bi exhibit its own local pztc? In terms of free charge, the pzfc of Bi lies at more negative values than the potential of the step adsorption peak of the clean platinum surface in the hydrogen region [51]. This means that in theory, the bismuth should exhibit a positive free charge at the potentials investigated in the present study and this should be compensated by electrolyte species such as water dipoles and anions. In fact in UHV, Bi adsorption on Pt{111} causes a decrease in the work function of the surface due to the difference in electronegativities between Bi and Pt [35] and this would be consistent with pzfc data for both elements [51]. However the amount of charge stored at Bi adatom sites would depend critically on the capacitance of these step adatoms. If this amount of stored charge is relatively low, very little electronic perturbation of adjacent terrace sites is expected. In this context, the lack of reactivity towards N_2O may be due simply to blocking of Bi sites by these electrostatically adsorbed species or poor activation of N_2O by bismuth. Similarly, one could argue that the reason CO displacement does not “see” charge at Bi sites is because in order to displace charge, CO must strongly chemisorb on bismuth (it does not). The lack of electronic modification in residual terrace sites however, argues against substantial charges accumulating at bismuth modified step sites. Whatever the real situation, only nitrous oxide reduction on the terrace is observed and so in this case “overall” and “local” pztc are equivalent. More importantly, it emphasises once again that if any correlation is to be sought between the UHV work function and electrochemical data (for example experimentalists being able to determine accurate changes in work function in an electrochemical cell rather than using a vacuum system), one must determine values of the pzfc, not the pztc since the large pseudocapacitances associated with chemisorption on Pt group metals would preclude direct comparisons between work function and pztc.

So why are global and local values of pztc useful and important in electrochemistry? There are several answers to this question. The first has been indicated previously. If pztc values are determined, by assuming models first postulated by Frumkin [3,13], it is possible subsequently to estimate pzfc values and thence compare with trends observed using work function data [52]. Hence fundamental insight into similarities and differences between adsorption in both environments may be obtained. The second answer lies in considerations of the “patchwork” nature of localised charged states at real electrochemical interphases (the co-existence of negative and positive total charges for certain ranges of potential on stepped surfaces has already been alluded to above). If electrocatalysis corresponds to adsorption followed by bond activation and these processes are potential dependent in the double layer environment, then access to the surface by reactive solution species

will be controlled by the adsorption/desorption of double layer components whose coverage in turn is determined by the total charge. This is why almost all electrochemical reactions are structure sensitive even though in UHV, for the same molecule, little structural sensitivity is usually observed [53–55]. At local values of pztc (not necessarily just of the clean surface but also of the surface containing some chemisorbed molecular intermediates), adsorption should be maximal since site blocking by double layer components is minimal. A good example of this effect is seen with methanol adsorption on Pt{100} whereby the maximum rate of (initial) dissociative chemisorption is situated at a potential roughly consistent with the location of the pztc of this surface [56]. Third, if the charge at the surface is important in activating water molecules to initiate surface electrooxidation, then both the pztc and the capacitance of the surface as a function of potential (hence the degree of charge accumulation at a particular local site) will be critical to this process. The onset of electrochemical oxide formation at step sites prior to terrace sites is clearly a manifestation of these concepts [57] and preferential etching of step sites relative to terraces by iodine at palladium surfaces [58,59] may be another. The onset of reaction between activated water/OH and chemisorbed species at potentials associated with different pztc's should also be reflected in discrete electrooxidation peaks associated with these regions. The changes in the onset of formic acid oxidation in the presence and absence of palladium on platinum and gold is illustrative in this regard [60,61]. Within the present study, the discrete local pztc of Pd islands on Pt{100} and Pd free regions would account readily for this behaviour and the difference in the onset potential of oxidation is predicted to be very close to the differences in their pztc's. It is tempting to assert, based on such correlations, that in fact electrooxidation can proceed *only* at potentials > local pztc. Future studies will be directed towards exploring further this assertion and also the role of total charge in electrocatalytic behaviour.

4. Conclusions

In order to extend our recent approach of utilising CO charge displacement and nitrous oxide reduction kinetics in tandem to elucidate overall and local values of the pztc [1], three more systems have been studied illustrating the utility of the method: a series of stepped Pt surfaces based on the $[01\bar{1}]$ zone, a Bi decorated Pt{332} surface and submonolayer amounts of palladium adsorbed on Pt{100}. For the stepped Pt electrodes, a linear decrease of overall pztc with step density was observed. N₂O reduction demonstrated that a Smoluchowski effect was operative whereby constant

values of local pztc for step and terrace sites, irrespective of step density, were evaluated. This finding contrasted with results obtained for stepped surfaces in the $[1\bar{1}0]$ zone [1].

For Bi decorated Pt{332}, a shift to more positive values of the pztc relative to the clean surface was observed. N₂O reduction indicated that the absence of a charge density associated with the step was the reason for this behaviour and in this particular case, the overall pztc was equal to the pztc of the residual {111} terrace sites. Negligible electronic perturbation of terrace sites by Bi adsorbed in step sites was found.

Finally, for Pd/Pt{100}, a gradual decrease in overall pztc as a function of Pd coverage up to 0.5 monolayers was seen followed by a more rapid decrease. The ability of N₂O to distinguish between clean surface, first monolayer and second monolayer (not reported here) palladium values of local pztc's may in future allow for a detailed examination of the electrocatalytic behaviour of the surface in terms of the number and onset potentials of various oxidation peaks. This will be the subject of future studies.

Acknowledgements

JMF thanks the Generalitat Valenciana for the funding through project GRUPOS03/208. GAA acknowledges the EPSRC (grant number M65724) for financial support and the Saudi Arabian Government for a studentship to OH. VC gratefully acknowledges the European Commission for the award of a Marie Curie Fellowship under contract number HPMF-CT-2002-01844.

References

- [1] V. Climent, G.A. Attard, J.M. Feliu, *J. Electroanal. Chem.* 532 (2002) 67.
- [2] V. Climent, E. Herrero, J.M. Feliu, *Electrochem. Commun.* 3 (2001) 590.
- [3] A.N. Frumkin, O.A. Petrii, B.B. Damaskin, in: J.O'M. Bockris, B.E. Conway, E. Yeager (Eds.), *Comprehensive Treatise of Electrochemistry*, vol. 1, Plenum Press, New York, 1980, p. 221 (Chapter 5).
- [4] J.O'M. Bockris, S.D. Argade, E. Gileadi, *Electrochim. Acta* 14 (1969) 1259.
- [5] A. Hamelin, in: B.E. Conway, R.E. White, J.O'M. Bockris (Eds.), *Modern Aspects of Electrochemistry*, vol. 16, Plenum Press, New York, 1985, p. 1 (Chapter 1).
- [6] J. Clavilier, in: A. Wieckowski (Ed.), *Interfacial Electrochemistry*, Marcel Dekker, New York, 1999 (Chapter 14).
- [7] G.A. Attard, A. Ahmadi, *J. Electroanal. Chem.* 389 (1995) 175.
- [8] V. Climent, R. Gómez, J.M. Orts, A. Aldaz, J.M. Feliu, in: C. Korzeniewski, B.E. Conway (Eds.), *The Electrochemical Society Proceedings (Electrochemical Double Layer)*, vol. 97-17, The Electrochemical Society, Pennington, NJ, 1997, p. 222.
- [9] V. Climent, R. Gómez, J.M. Feliu, *Electrochim. Acta* 45 (1999) 629.

- [10] R. Gómez, V. Climent, J.M. Feliu, M.J. Weaver, *J. Phys. Chem. B* 104 (2000) 597.
- [11] U.W. Hamm, D. Kramer, R.S. Zhai, D.M. Kolb, *J. Electroanal. Chem.* 414 (1996) 85.
- [12] T. Pajkossy, D.M. Kolb, *Electrochim. Acta* 46 (2001) 3063.
- [13] A.N. Frumkin, O.A. Petrii, *Electrochim. Acta* 20 (1975) 347.
- [14] J. Clavilier, D. Armand, S.-G. Sun, M. Petit, *J. Electroanal. Chem.* 205 (1986) 267.
- [15] E. Herrero, J.M. Orts, A. Aldaz, J.M. Feliu, *Surf. Sci.* 440 (1999) 259.
- [16] A. Al-Akl, G.A. Attard, R. Price, B. Timothy, *J. Electroanal. Chem.* 467 (1999) 60.
- [17] A. Al-Akl, G. Attard, R. Price, B. Timothy, *Phys. Chem. Chem. Phys.* 3 (2001) 3261.
- [18] L.A. Kibler, A. Cuesta, M. Kleinert, D.M. Kolb, *J. Electroanal. Chem.* 484 (2000) 73.
- [19] J. Clavilier, M.J. Llorca, J.M. Feliu, A. Aldaz, *J. Electroanal. Chem.* 310 (1991) 429.
- [20] M.J. Llorca, J.M. Feliu, A. Aldaz, J. Clavilier, *J. Electroanal. Chem.* 351 (1993) 299.
- [21] B. Alvarez, A. Berná, A. Rodes, J.M. Feliu, *Surf. Sci.* (submitted).
- [22] J. Clavilier, R. Albalat, R. Gómez, J.M. Orts, J.M. Feliu, *J. Electroanal. Chem.* 360 (1993) 325.
- [23] K. Wandelt, *Appl. Surf. Sci.* 111 (1997) 1.
- [24] J.F. Jia, K. Inoue, Y. Hasegawa, W.S. Yang, T. Sakurai, *J. Vac. Sci. Technol. B* 15 (1997) 1861.
- [25] R. Smoluchowski, *Phys. Rev.* 60 (1941) 661.
- [26] K.B. Besocke, B. Krahl-Urban, H. Wagner, *Surf. Sci.* 68 (1977) 39.
- [27] J. Lecoœur, J. Andro, R. Parsons, *Surf. Sci.* 114 (1982) 320.
- [28] S. Motoo, N. Furuya, *Ber. Bunsenges. Phys. Chem.* 91 (1987) 457.
- [29] N.M. Markovic, N.S. Marinkovic, R.R. Adzic, *J. Electroanal. Chem.* 241 (1988) 309.
- [30] A. Rodes, K. El Achi, M.A. Zamakhchari, J. Clavilier, *J. Electroanal. Chem.* 284 (1990) 245.
- [31] K. Domke, E. Herrero, A. Rodes, J.M. Feliu, *J. Electroanal. Chem.* 552 (2003) 115.
- [32] J.M. Orts, R. Gómez, J.M. Feliu, A. Aldaz, J. Clavilier, *Electrochim. Acta* 39 (1994) 1519.
- [33] M. Wakisaka, M. Sugimasa, J. Inukai, K. Itaya, *J. Electrochem. Soc.* 150 (2003) E81.
- [34] E. Herrero, V. Climent, J.M. Feliu, *Electrochem. Commun.* 2 (2000) 636.
- [35] M.T. Paffett, C.T. Campbell, T.N. Taylor, *J. Chem. Phys.* 85 (1986) 6176.
- [36] G.A. Attard, A. Bannister, *J. Electroanal. Chem.* 300 (1991) 467.
- [37] G.A. Attard, R. Price, A. AlAkl, *Electrochim. Acta* 34 (1994) 1525.
- [38] G.A. Attard, R. Price, *Surf. Sci.* 335 (1995) 63.
- [39] B. Alvarez, V. Climent, A. Rodes, J.M. Feliu, *J. Electroanal. Chem.* 497 (2001) 125.
- [40] B. Alvarez, V. Climent, A. Rodes, J.M. Feliu, *Phys. Chem. Chem. Phys.* 3 (2001) 3269.
- [41] B. Alvarez, A. Rodes, J.M. Perez, J.M. Feliu, J.L. Rodriguez, E. Pastor, *Langmuir* 16 (2000) 4695.
- [42] L.A. Kibler, M. Kleinert, R. Randler, D.M. Kolb, *Surf. Sci.* 443 (1999) 19.
- [43] L.A. Kibler, M. Kleinert, D.M. Kolb, *Surf. Sci.* 461 (2000) 155.
- [44] L.A. Kibler, M. Kleinert, V. Lazarescu, D.M. Kolb, *Surf. Sci.* 498 (2002) 175.
- [45] V. Climent, N.M. Markovic, P.N. Ross, *J. Phys. Chem. B* 104 (2000) 3116.
- [46] N.M. Markovic, C.A. Lucas, V. Climent, V. Stamenkovic, P.N. Ross, *Surf. Sci.* 465 (2000) 103.
- [47] H. Naohara, S. Ye, K. Uosaki, *J. Phys. Chem. B* 102 (1998) 4366.
- [48] H. Naohara, S. Ye, K. Uosaki, *Colloids Surf. A* 154 (1999) 201.
- [49] H. Naohara, S. Ye, K. Uosaki, *J. Electroanal. Chem.* 473 (1999) 2.
- [50] B. Alvarez, Thesis, Universidad de Alicante, Alicante, 2001.
- [51] S. Trasatti, E. Lust, in: R.E. White, J.O'M. Bockris, B.E. Conway (Eds.), *Modern Aspects of Electrochemistry*, vol. 33, Kluwer Academic/Plenum Publishers, New York, 1999, p. 1 (Chapter 1).
- [52] M.J. Weaver, *Langmuir* 14 (1998) 3932.
- [53] G.A. Attard, K. Chibane, H.D. Ebert, R. Parsons, *Surf. Sci.* 224 (1989) 311.
- [54] N. Kizhakevariam, E.M. Stuve, *Surf. Sci.* 286 (1993) 246.
- [55] D.H. Ehlers, A. Spitzer, H. Luth, *Surf. Sci.* 160 (1985) 57.
- [56] E. Herrero, K. Franaszczuk, A. Wieckowski, *J. Phys. Chem.* 98 (1994) 5074.
- [57] J. Narayanasamy, A.B. Anderson, *J. Electroanal. Chem.* 554 (2003) 35.
- [58] K. Sashikata, Y. Matsui, K. Itaya, M.P. Soriaga, *J. Phys. Chem.* 100 (1996) 20027.
- [59] Y.G. Kim, M.P. Soriaga, *J. Phys. Chem. B* 102 (1998) 6188.
- [60] M.J. Llorca, J.M. Feliu, A. Aldaz, J. Clavilier, *J. Electroanal. Chem.* 376 (1994) 151.
- [61] M. Baldauf, D.M. Kolb, *J. Phys. Chem.* 100 (1996) 11375.